Implementation of standard quantum error-correction codes for solid-state qubits

Tetsufumi Tanamoto

Corporate R & D Center, Toshiba Corporation, Saiwai-ku, Kawasaki 212-8582, Japan

In quantum error-correcting code (QECC), many quantum operations and measurements are necessary to correct errors in logical qubits. In the stabilizer formalism, which is widely used in QECC, generators G_i ($i = 1, 2, \ldots$) consist of multiples of Pauli matrices and perform encoding, decoding, and measurement. In order to maintain encoding states, the stabilizer Hamiltonian $H_{\mathrm{stab}} = -\sum_i G_i$ is suitable because its ground state corresponds to the code space. On the other hand, Hamiltonians of most solid-state qubits have two-body interactions and show their own dynamics. In addition solid-state qubits are fixed on substrate and qubit-qubit operation is restricted in their neighborhood. The main purpose of this paper is to show how to directly generate the stabilizer Hamiltonian H_{stab} from conventional two-body Hamiltonians with Ising interaction and XY interaction by applying a pulse control method such as an NMR technique. We show that generation times of H_{stab} for nine-qubit code, five-qubit code, and Steane code are estimated to be less than 300 ns when typical experimental data of superconducting qubits are used, and sufficient pulse control is assumed. We also show how to prepare encoded states from an initial state $|0, \ldots, 0\rangle$. In addition, we discuss an appropriate arrangement of two- or three-dimensional arrayed qubits.

I. INTRODUCTION

Similar to the digital computer, a rigid error-correcting system is required in the quantum computer. Various quantum error-correcting codes (QECC) have been developed such as the standard code [1–9], the subsystem codes [10–12], and the topological code [13–18]. In QECC, it is necessary for many qubits to be coherently entangled for constructing logical qubits. For instance, nine qubits are required for a logical qubit of the nine-qubit code [1], seven qubits are required for the seven-qubit Steane code, which is the smallest code of the general CSS code [2], and so on [3,4]. In any quantum codes, many operations and measurements are required for encoding, decoding, and error-correcting processes. There are strict requirements concerning the maximum error rate for the success of QECC [3–5,18]. All manipulations of many qubits should be done sufficiently within the coherence time.

In general, it is difficult to produce desired encoded states consisting of many qubits. However, it is also difficult to maintain each entangled state during the time required in a flow of quantum computation [6–9]. This problem arises when the encoded state is not the eigenstate of a system Hamiltonian. The encoded state changes following the dynamics of the system Hamiltonian. Assume that a computer system consists of many blocks. Each block must correlate with every other block to carry out a definite set of quantum computations. As a simple structure of a computing system, let us consider a system in which operations are synchronized to a system clock, which is the case with the present widely used digital computers. Then, all operations are carried out step by step as the system clock ticks the system time. Entangled states produced by controlled-NOT (CNOT) gates or other quantum gates appear only periodically when the entangled states are not the ground states of the system Hamiltonian. In such case, if each block of a system includes an individual entangled state, it will be difficult to control the synchronization of the total system because the period of the desired entangled states

differs depending on the dynamics of each block. Thus, it will be desirable for encoded states to be the ground states of Hamiltonians of the blocks. Moreover, because each block of a system changes its role as system time passes, it is desirable that the Hamiltonian of each block changes depending on each calculation step.

In this paper, we show how to efficiently implement standard QECC in solid-state qubit systems with natural two-body interactions, focusing on the stabilizer formalism. Stabilizer operators $\{G_i | 1 \leqslant i \leqslant l\}$ are mutually commuting operators given by products of multiple Pauli matrices [3,4]. Logical qubit states are encoded into a mutual eigenspace $\mathcal{H}_S$ of dimension 2^l of these operators through measurements. For l different stabilizers and n physical qubits, a maximum number of $k = n - l$ logical qubits can be encoded into $\mathcal{H}_S$, whereas $k < n - l$ in the case of subsystem encoding [10–12]. Although preparation of some "quantum memory" blocks to where logical qubit states can be transferred or teleported is one solution to preserve logical qubit states, we consider that it is better to change a system Hamiltonian into a stabilizer Hamiltonian defined by $H_{\mathrm{stab}} \equiv -\sum_i G_i$, because transformation or teleportation of encoded states requires more complexity. We would also like to show how to generate encoded states without measurements. The encoded states are generated by using operators that are modified from stabilizer operators. Therefore, in this paper, we mainly describe the generation process of H_{stab}.

In previous papers [19,20], we showed that we can construct G_i one by one based on the two-body Hamiltonian by using the appropriate pulse sequence. However, it is much more efficient to directly produce H_{stab}. In this paper, we show how to directly create H_{stab} starting from the two-body Hamiltonian. H_{stab} has a complicated form of multiplied Pauli matrices. We show that appropriate pulse sequences to generate H_{stab} can be found by inversely tracing a transformation from H_{stab} into a single-qubit Hamiltonian that can be obtained when the qubits are decoupled by an initial pulse sequence by suppressing
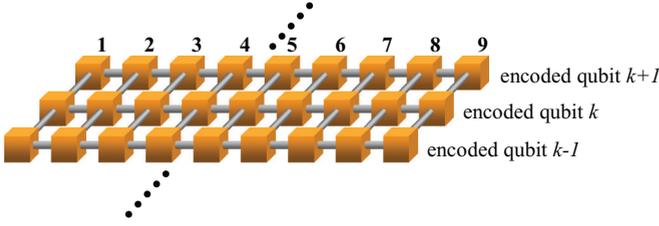
FIG. 1. (Color online) Two-dimensional qubit array aiming at Shor's nine-qubit code. Boxes show qubits and bars between the boxes show interactions between qubits. Horizontal qubits constitute logical qubits.

the interaction terms. We show that the direct creation of H_{stab} greatly reduces the number of operations compared with our previous method in Refs. [19,20]. This reduction is remarkable in the case of qubits with XY interaction. For example, the number of single-qubit rotations N_{rot} and that of qubit-qubit XY interaction N_{int} are reduced from $N_{\text{rot}} = 44$ to $N_{\text{rot}} = 20$, and from $N_{\text{int}} = 288$ to $N_{\text{int}} = 132$, respectively, for the Steane code. Similar results are obtained for the nine-qubit code and the five-qubit code. Accordingly, operation time can also be reduced. If we use a typical experimental parameter of superconducting qubits, we can reduce the time required to generate H_{stab} by 48.4% (194 ns), 59.1% (127.5 ns), and 54.4% (257 ns) for the nine-qubit code, the five-qubit code, and the Steane code, respectively. The present method has the advantage that, as pulse control technology progresses, pulse error rate and speed are improved. Pulse errors can be corrected by using NMR techniques such as the composite-pulse method [21–25], and the speed is increased by improving a control system operated by a digital computer.

We also investigate a possible architecture of standard codes for solid-state qubits on lattice sites. In general, interactions between solid-state qubits are restricted to their nearest-neighbor or next-nearest-neighbor sites [26–32]. In order to prevent unexpected external noise, it is preferable for physical qubits in a logical qubit to be placed compactly in a small region. Moreover, for logical qubits to interact effectively with one another, it is desirable to place logical qubits side by side. Therefore, it is natural to construct logical qubit by one-dimensional (1D) qubit arrays and place them parallel as shown in Fig. 1. In addition, frequent measurements in QECC require other qubit arrays for measurements. We will discuss possible setups of a qubit system.

This paper is organized as follows: In Sec. II we establish the general procedure of generating the stabilizer Hamiltonian. In Sec. III, we show examples of generating the stabilizer Hamiltonian in the standard code, and in Sec. IV we show how to generate the code state. Finally, in Sec. V, we consider possible qubit architecture realized by solid-state qubits. We close with a summary and conclusions in Sec. VII.

II. STABILIZER HAMILTONIAN GENERATION METHOD

A. Stabilizer coding and stabilizer Hamiltonian

In the stabilizer code [3,4], encoding, decoding, and error correction are carried out based on the stabilizers, which

are mutually commutable and can be expressed by the Pauli matrices:

$$G_l = \otimes_{i=1}^{n} (X_i)^{x_i(G_l)} (Z_i)^{z_i(G_l)} \tag{1}$$

[$x_i(G_l)$, $z_i(G_l) \in \{0,1\}$], where Pauli matrices are given by

$$X = \begin{pmatrix} 0 & 1 \\ 1 & 0 \end{pmatrix}, \quad Y = \begin{pmatrix} 0 & -i \\ i & 0 \end{pmatrix}, \quad Z = \begin{pmatrix} 1 & 0 \\ 0 & -1 \end{pmatrix}. \tag{2}$$

The code word $|\Psi_m\rangle$ obeys the eigenvalue equation

$$G_l|\Psi_m\rangle = |\Psi_m\rangle. \tag{3}$$

Conventionally, in order to construct encoding states, starting from an initial state $\Pi_{i=1}^{k}|0\rangle_i$, measurements over stabilizer operators of the selected code are repeated. Depending on the measurement outcome, the common eigenstate is fixed to be the desirable encoded state. The correction procedure for the stabilizer code is carried out by measuring all relevant stabilizer operators.

The stabilizer Hamiltonian H_{stab} is defined by

$$H_{\text{stab}} = -\sum_{i=1}^{l} G_i, \tag{4}$$

where the summation is taken over the constituent stabilizers of each code. Owing to the commutability of the stabilizers G_i, the ground state of Eq. (4) is a common eigenstate of the stabilizers, which is the encoded logical state. For the sake of simplicity, we consider the standard codes without considering the subsystem code ($k = n - l$).

B. System Hamiltonian

The solid-state Hamiltonian controlled by pulse signals can be written as [33–35]

$$H(t) = \sum_i \left[\Omega_{0i} Z_i + 2\Omega_i \cos\left(\omega_i^{\text{rf}} t + \delta_i\right) X_i \right] + \sum_{i<j} J_{ij} X_i X_j, \tag{5}$$

where Ω_i and ω_i^{rf} are an amplitude and a frequency of a controlled signal applied to a qubit i. If we move to a frame rotating with the radio frequency ω_i^{rf} about the z axis, $H^r = R^{-1} H(t) R$, with $R = \exp[-i \sum_i (\omega_i^{\text{rf}} t/2) Z_i]$, then the transferred static Hamiltonian $H' = H^r - \sum_i (\omega_i^{\text{rf}} t/2) Z_i$ is approximately given by

$$H' = \sum_i \left[\left(\Omega_{0i} - \frac{\omega_i^{\text{rf}}}{2} \right) Z_i + \Omega_i (\cos \delta_i X_i - \sin \delta_i Y_i) \right] + \sum_{i<j} \frac{J_{ij}}{2} [X_i X_j + Y_i Y_j] \tag{6}$$

(high-frequency components $2\omega_i^{\text{rf}}$ can be neglected). If Eq. (5) includes an interaction of $\sum_{i<j} J_{ij} Z_i Z_j$ instead of $\sum_{i<j} J_{ij} X_i X_j$, the final Hamiltonian, Eq. (6), includes the Ising interaction. The x pulse and y pulse for qubit i are realized when $\delta = 0$ and $\delta = -\pi/2$ signals are respectively applied to the qubit with $\omega_i^{\text{rf}} = 2\Omega_{0i}$. We assume that each pulse is sufficiently strong for interactions between qubits to be neglected during the pulse sequences ($\Omega_i, \Omega_{0i} > J_{ij}$).

Then the qubit Hamiltonian in the rotating frame of $\omega_i^{\mathrm{rf}} = 2\Omega_{0i}$ is expressed by

$$H_q = H_0 + H_{\mathrm{int}}, \qquad (7)$$

where a single-qubit part H_0 is given by

$$H_0 = \sum_i H_{0i} = \sum_i \Omega_i X_i. \qquad (8)$$

The interacting part $H_{\mathrm{int}} = \sum_{ij} H_{\mathrm{int}}^{ij}$ is expressed by

$$H_{XY} = \sum_{i<j} H_{XY}^{ij} = \sum_{i<j} J_{ij}[X_i X_j + Y_i Y_j], \qquad (9)$$

for XY interaction, and

$$H_{\mathrm{Ising}} = \sum_{i<j} H_{\mathrm{Ising}}^{ij} = \sum_{i<j} J_{ij} Z_i Z_j, \qquad (10)$$

for Ising interaction.

C. Dynamic generation of stabilizer Hamiltonian

The generation of H_{stab} from a qubit Hamiltonian H_q consists of two steps. The first step is to extract a single-qubit part or a pure two-body interaction part from H_q. The second step is to construct H_{stab} dynamically with pulse sequences by using a selected single-qubit part H_{ini} and qubit-qubit interactions H_{int}^{ij}. Because the second step is the core framework of this paper, we first describe the second step of dynamical transformation to H_{stab}. The extraction method is described in Sec. II D.

The transformation from the two-body Hamiltonian H_q to the many-body Hamiltonian H_{stab} is carried out dynamically by using a time evolution of a system starting from a simple initial Hamiltonian $H_{\mathrm{ini}} \propto X_i, Y_i$, or Z_i [19,20]. The time evolution of the generation process is illustrated with the schematic notation $\rho(0) \xrightarrow{tH} \rho(t)$, where $\rho(t) = \exp(-iHt)\rho(0)\exp(iHt)$ is the density matrix for a time-independent Hamiltonian H, or for an effective H in the sense of the average Hamiltonian theory [21]. After the application of mutually inverse, unitary operations according to

$$\rho(0) \xrightarrow{\tau_{\mathrm{op}} H_{\mathrm{op}}} \xrightarrow{\tau_{\mathrm{ini}} H_{\mathrm{ini}}} \xrightarrow{-\tau_{\mathrm{op}} H_{\mathrm{op}}} \rho(\tau_{\mathrm{ini}} + 2\tau_{\mathrm{op}}), \qquad (11)$$

the system evolves as if propagated by the effective Hamiltonian $\exp(-i\tau_{\mathrm{op}} H_{\mathrm{op}})H_{\mathrm{ini}}\exp(i\tau_{\mathrm{op}} H_{\mathrm{op}})$ for a time τ_{ini} [19]. Here, H_{op} is an operator by which an initial Hamiltonian is changed into the target effective Hamiltonian.

To build H_{stab} from H_{ini}, we need two elementary transformations for H_{op} in Eq. (11): one that rotates arbitrary single-qubit terms through an angle of $\pi/2$ and another that increases the order of Pauli-matrix terms by one. Higher-order products of Pauli matrices can be generated using the following transformations [19]:

$$e^{-i\theta[XY]_{12}} X_1 e^{i\theta[XY]_{12}} = \cos(2\theta)X_1 - \sin(2\theta)Z_1 Y_2, \quad (12)$$

$$e^{-i\theta[XY]_{12}} Y_1 e^{i\theta[XY]_{12}} = \cos(2\theta)Y_1 + \sin(2\theta)Z_1 X_2, \quad (13)$$

$$e^{-i\theta[XY]_{12}} Z_1 e^{i\theta[XY]_{12}} = \cos^2(2\theta)Z_1 + \sin^2(2\theta)Z_2$$
$$+ \tfrac{1}{2}\sin(4\theta)[X_1 Y_2 - Y_1 X_2], \quad (14)$$

for XY interaction. When $\theta = \pi/4$ we can change the number of Pauli matrices given by

$$X_1 \rightarrow -Z_1 Y_2, \qquad (15)$$

$$Y_1 \rightarrow Z_1 X_2, \qquad (16)$$

$$Z_1 \rightarrow Z_2. \qquad (17)$$

For Ising interaction, we use the relations given by

$$e^{-i\theta Z_1 Z_2} X_1 e^{i\theta Z_1 Z_2} = \cos(2\theta)X_1 + \sin(2\theta)Y_1 Z_2, \qquad (18)$$

$$e^{-i\theta Z_1 Z_2} Y_1 e^{i\theta Z_1 Z_2} = \cos(2\theta)Y_1 - \sin(2\theta)X_1 Z_2. \qquad (19)$$

Then, for $\theta = \pi/4$, we can change the number of Pauli matrices given by

$$X_1 \rightarrow Y_1 Z_2, \qquad (20)$$

$$Y_1 \rightarrow -X_1 Z_2, \qquad (21)$$

$$Z_1 \rightarrow Z_1. \qquad (22)$$

By combining these equations with single-qubit rotations, we can change H_q to H_{stab}.

D. Extracting H_{ini} and H_{int}^{ij} from a qubit Hamiltonian

In order to use the above-mentioned dynamic method, the important step is to extract a single-qubit part or a pure two-body interaction part from a qubit Hamiltonian H_q. This process is carried out using the Baker-Campbell-Hausdorff (BCH) formula [21]. Here, we assume that qubits interact with their nearest-neighbor qubits. Then, in order to define a logical qubit, we have to determine the locations of physical qubits in a logical qubit. In this section, after we explain the BCH formula, we would like to define a logical qubit arranged on lattice sites. Then, finally we will show how to extract a single-qubit part H_{ini} and a pure two-body interaction H_{op} from the Hamiltonian of a qubit lattice.

1. Manipulation by using the BCH formula

A desirable part of the original Hamiltonian H_q is extracted by using appropriate pulse sequences [19]. The basic idea can be illustrated by using the standard NMR Hamiltonian $H_{\mathrm{NMR}} = \sum_i \varepsilon_i Z_i + \sum_{i<j} J Z_i Z_j$. In this case, because of the property $[H_0, H_{\mathrm{int}}] = 0$, H_0 and H_{int} can be separately obtained by using a simple pulse sequence. The interaction part H_{Ising} can be extracted by using two sandwiched π pulses such as $\exp(i\tau H_{\mathrm{Ising}}) = e^{-i(\pi/2)\sum_j Y_j} e^{i(\tau/2)H_{\mathrm{NMR}}} e^{i(\pi/2)\sum_j Y_j} e^{i(\tau/2)H_{\mathrm{NMR}}}$. For the general Hamiltonian [Eqs. (8)–(10)], because $[H_0, H_{\mathrm{int}}] \neq 0$, we approximately obtain a desirable part by repeatedly applying the BCH formula. For $A = h_a + h_b$ (original Hamiltonian) and $B = h_a - h_b$ (transferred by applying a π pulse) with $h_a = i\tau H_a$ and $h_b = i\tau H_b$, we can extract $h_a = i\tau H_a$ by using the relation given by

$$(e^A e^B)^n \approx \exp\left[i2t_0 H_a + \left(t_0^2/n\right)[H_a, H_b]\right] \qquad (23)$$

($t_0 \equiv n\tau$). Thus, as long as $(t_0/n)||H_b|| \ll 1$ where $||A|| = [\text{Tr}(A^\dagger A)/d]^{1/2}$ is the standard operator norm in a Hilbert space of dimension d, we can neglect the second term. As the number n of repetitions increases, this approximation improves.

In the following sections, we use an extended form of Eq. (23) described by

$$
\begin{aligned}
(e^A e^B e^{B'} e^{A'})^n &\approx [\exp(2h_a + [h_b, h_a]) \exp(2h'_a - [h'_b, h'_a])]^n \\
&\approx \exp[2n(h_a + h'_a) + n[h_b, h_a] \\
&\quad - n[h'_b, h'_a] + 4n[h_a, h'_a]],
\end{aligned}
\tag{24}
$$

where $A' = h'_a + h'_b$ and $B' = h'_a - h'_b$. $2(h_a + h'_a)$ is the target Hamiltonian. In the following two sections, we show how to extract a desirable interaction term H_{int}^{ij} and a single-qubit part H_0 from H_q by using Eq. (24).

2. Qubit lattice and logical qubit

We consider a qubit lattice in which physical qubits are arrayed on a lattice site interacting with their neighboring qubits. The simplest arrangement is a 1D array as shown in Fig. 1. Then we can interact logical qubits with their nearest-neighbor logical qubits by using interactions between physical qubits. The number of qubits in each 1D array depends on how many physical qubits are required to construct a single logical qubit. In Fig. 1, nine qubits constitute a logical qubit.

3. Selection of a single-qubit Hamiltonian

Here we show how to extract H_0 from H_q for two-dimensional (2D) qubit lattice, assuming always-on interactions between qubits. As an example, we consider logical qubits consisting of five qubits. In a 1D qubit array, H_0 is obtained by choosing $B = -h_1 + h_2 - h_3 + h_4 - h_5 - \sum_i h_{ij}$ and $B' = h_1 - h_2 + h_3 - h_4 + h_5 - \sum_i h_{ij}$, while A and A' are H_q in Eq. (24) [$h_i = \tau H_{0i}$ and $h_{ij} = \tau H_{\text{int}}^{ij}$]. This procedure can be extended to the 2D lattice case by taking into account interactions between different logical qubits.

In this section, we treat Hamiltonians that include two types of Pauli matrices or fewer, such as Eq. (5) or Eq. (6), with $\omega_i^{\text{rf}} = 2\Omega_{0i}$. For Eq. (5), "$\pi$ pulse" corresponds to a π pulse around the y axis. For Eq. (6) with $\omega_i^{\text{rf}} = 2\Omega_{0i}$, "$\pi$ pulse" corresponds to a π pulse around the z axis, which can also be produced by a π pulse around the y axis after that around the x axis. Extraction of H_0 and two-body interaction from the Hamiltonian, Eq. (6), with $\omega_i^{\text{rf}} \neq 2\Omega_{0i}$ is described in Appendix A.

The 2D lattice Hamiltonian is given by

$$
H^{\text{2D}} = \sum_k H_q^{(k)},
\tag{25}
$$

where

$$
H_q^{(k)} = H_0^{(k)} + H_{\text{int}}^{(k)} + H_{\text{int}}^{(k,k+1)}.
\tag{26}
$$

$H_{\text{int}}^{(k,k+1)}$ shows an interaction term between kth logical qubits and $(k+1)$th qubits. In order to separate different logical qubits, $H_{\text{int}}^{(k,k+1)}$ should be erased. We apply π pulses to (i) qubits 1,3,5 of $\ldots,(k-1)$th,$(k+1)$th,$\ldots$ arrays for A; (ii) qubits 1,3,5 of $\ldots,k$th,$(k+2)$th,$\ldots$ arrays for B; (iii) qubits 2,4 of $\ldots,(k-1)$th,$(k+1)$th,$\ldots$ arrays for B'; and

(iv) qubits 2,4 of qubits of $\ldots,k$th,$(k+2)$th,$\ldots$ arrays for A':

$$
\begin{aligned}
A = &\cdots - h_1^{(k-1)} + h_2^{(k-1)} - h_3^{(k-1)} + h_4^{(k-1)} - h_5^{(k-1)} - h_{\text{int}}^{(k-1)} \\
&- h_{11}^{(k-1,k)} + h_{22}^{(k-1,k)} - h_{33}^{(k-1,k)} + h_{44}^{(k-1,k)} - h_{55}^{(k-1,k)} \\
&+ h_q^{(k)} - h_{11}^{(k,k+1)} + h_{22}^{(k,k+1)} - h_{33}^{(k,k+1)} + h_{44}^{(k,k+1)} \\
&- h_{55}^{(k,k+1)} - h_1^{(k+1)} + h_2^{(k+1)} - h_3^{(k+1)} + h_4^{(k+1)} - h_5^{(k+1)} \\
&- h_{\text{int}}^{(k+1)} \cdots,
\end{aligned}
\tag{27}
$$

$$
\begin{aligned}
B = &\cdots + h_q^{(k-1)} - h_{11}^{(k-1,k)} + h_{22}^{(k-1,k)} - h_{33}^{(k-1,k)} + h_{44}^{(k-1,k)} \\
&- h_{55}^{(k-1,k)} - h_1^{(k)} + h_2^{(k)} - h_3^{(k)} + h_4^{(k)} - h_5^{(k)} - h_{\text{int}}^{(k)} \\
&- h_{11}^{(k,k+1)} + h_{22}^{(k,k+1)} - h_{33}^{(k,k+1)} + h_{44}^{(k,k+1)} - h_{55}^{(k,k+1)} \\
&+ h_q^{(k+1)} \cdots,
\end{aligned}
\tag{28}
$$

$$
\begin{aligned}
B' = &\cdots + h_1^{(k-1)} - h_2^{(k-1)} + h_3^{(k-1)} - h_4^{(k-1)} + h_5^{(k-1)} - h_{\text{int}}^{(k-1)} \\
&+ h_{11}^{(k-1,k)} - h_{22}^{(k-1,k)} + h_{33}^{(k-1,k)} - h_{44}^{(k-1,k)} + h_{55}^{(k-1,k)} \\
&+ h_q^{(k)} + h_{11}^{(k,k+1)} - h_{22}^{(k,k+1)} + h_{33}^{(k,k+1)} - h_{44}^{(k,k+1)} \\
&+ h_{55}^{(k,k+1)} + h_1^{(k+1)} - h_2^{(k+1)} + h_3^{(k+1)} - h_4^{(k+1)} + h_5^{(k+1)} \\
&- h_{\text{int}}^{(k+1)} \cdots,
\end{aligned}
\tag{29}
$$

$$
\begin{aligned}
A' = &\cdots + h_q^{(k-1)} + h_{11}^{(k-1,k)} - h_{22}^{(k-1,k)} + h_{33}^{(k-1,k)} - h_{44}^{(k-1,k)} \\
&+ h_{55}^{(k-1,k)} + h_1^{(k)} - h_2^{(k)} + h_3^{(k)} - h_4^{(k)} + h_5^{(k)} - h_{\text{int}}^{(k)} \\
&+ h_{11}^{(k,k+1)} - h_{22}^{(k,k+1)} + h_{33}^{(k,k+1)} - h_{44}^{(k,k+1)} + h_{55}^{(k,k+1)} \\
&+ h_q^{(k-1)} \cdots,
\end{aligned}
\tag{30}
$$

where $h_q^{(k)} = \tau(H_0^{(k)} + H_{\text{int}}^{(k)})$. By using Eq. (24), we obtain $H_{\text{eff}} = 2\sum_k H_0^{(k)}$.

4. Selection of two-body interaction

Next, we show how to extract the interaction term H_{int}^{ij} between two qubits in order to use Eqs. (12)–(14) or Eqs. (18) and (19) for the 2D lattice qubits. As an example, we consider a case of extracting $h_{23} = i\tau H_{\text{int}}^{23}$ in a five-qubit array. The required transformation is given by extending the results of Ref. [20]. A in Eq. (24) is the original Hamiltonian such as $A = \tau(H_0 + H_{\text{int}})$. B in Eq. (24) is given by applying a π pulse to qubits 2,3,5 of $(k+2n)$th logical qubits and qubits 1,4 of $(k+2n-1)$th logical qubits (n is an integer):

$$
\begin{aligned}
B = &\cdots - h_1^{(k-1)} + h_2^{(k-1)} + h_3^{(k-1)} - h_4^{(k-1)} + h_5^{(k-1)} \\
&- h_{12}^{(k-1)} + h_{23}^{(k-1)} - h_{34}^{(k-1)} - h_{45}^{(k-1)} - h_{\text{int}}^{(k-1,k)} \\
&+ h_1^{(k)} - h_2^{(k)} - h_3^{(k)} + h_4^{(k)} - h_5^{(k)} - h_{12}^{(k)} + h_{23}^{(k)} \\
&- h_{34}^{(k)} - h_{45}^{(k)} - h_{\text{int}}^{(k,k+1)} - h_1^{(k+1)} + h_2^{(k+1)} \\
&+ h_3^{(k+1)} - h_4^{(k+1)} + h_5^{(k+1)} - h_{12}^{(k+1)} + h_{23}^{(k+1)} \\
&- h_{34}^{(k+1)} - h_{45}^{(k+1)} - h_{\text{int}}^{(k+1,k+2)} \cdots,
\end{aligned}
\tag{31}
$$

where $h_i^{(k)} \equiv i\tau H_0^{(k)}$ and $h_{ij}^{(k)} = i\tau H_{int}^{(k)}$. B' is given by applying a π pulse to qubits 2,3,5 of $(k+2n-1)$th logical qubits and qubits 1,4 of $(k+2n)$th logical qubits (n is an integer):

$$
\begin{aligned}
B' = \cdots &+ h_1^{(k-1)} - h_2^{(k-1)} - h_3^{(k-1)} + h_4^{(k-1)} - h_5^{(k-1)} \\
&- h_{12}^{(k-1)} + h_{23}^{(k-1)} - h_{34}^{(k-1)} - h_{45}^{(k-1)} - h_{int}^{(k-1,k)} \\
&- h_1^{(k)} + h_2^{(k)} + h_3^{(k)} - h_4^{(k)} + h_5^{(k)} \\
&- h_{12}^{(k)} + h_{23}^{(k)} - h_{34}^{(k)} - h_{45}^{(k)} - h_{int}^{(k,k+1)} + h_1^{(k+1)} - h_2^{(k+1)} \\
&- h_3^{(k+1)} + h_4^{(k+1)} - h_5^{(k+1)} - h_{12}^{(k+1)} + h_{23}^{(k+1)} \\
&- h_{34}^{(k+1)} - h_{45}^{(k+1)} - h_{int}^{(k+1,k+2)} \cdots .
\end{aligned}
\tag{32}
$$

The A' is obtained by applying a π pulse to all qubits given by

$$
A' = \tau(-H_0 + H_{int}).
\tag{33}
$$

By using Eq. (24), we can obtain $\sum_k 4h_{23}^{(k)}$.

The perturbation terms in Eq. (24) are described in Appendix B. For the selection of $\sum_k 4h_{23}^{(k)}$, the perturbation is estimated as $||H_{pert}|| \approx 10\tau N_{qubit}J\Omega$, and for the case of H_0, we have $||H_{pert}|| \approx 20\tau N_{qubit}J\Omega$, where N_{qubit} is the number of connected qubits. As long as N_{qubit} is not large, these perturbation terms can be neglected by repeating Eq. (24) with $J_{ij}t_0/n \ll 1$. Hereafter, we consider the case of $n=1$ for simplicity. Note that the procedure described in this section can be easily extended to three-dimensionally (3D) arrayed qubits.

E. Estimation of elapsed time

In order to estimate an operation time of pulse manipulations, we express the time for single-qubit rotation as τ_{rot}. For preparing a single Hamiltonian H_0, it takes an extra time of $5\tau_{rot}$, because, in Eq. (24), four Hamiltonians A, B, B', and A' are transformed from H_q by being sandwiched by π pulses. It also takes extra times of $4\tau_{rot}$ and $5\tau_{rot}$ to obtain $\exp(i\tau_{op}H_{op})$ and $\exp(-i\tau_{op}H_{op})$, respectively, in Eq. (11). In the latter case, τ_{rot} is required to reverse the sign of H_{op}. Thus, for N_{op} qubit-qubit operations, it takes a time of $N_{op}[2\tau_{op} + 9\tau_{rot}]$.

In the following, we would like to address the feasibility of our scheme in a typical superconducting qubit system. Note that our qubit lattice model can be applied not only to solid-state coupling qubits [36–39], but also to circuit-QED qubits [40–43]. For two superconducting qubits in a circuit-QED setup the effective interqubit interaction can be treated as XY type [44,45]. For instance, for $g/\Delta = 0.1$, $g/(2\pi) = 200$ MHz, $\Delta/(2\pi) = 2$ GHz, where g is the Jaynes-Cummings coupling constant and Δ is the detuning between the resonator frequency and the qubit splitting, we have $J/(2\pi) = 20$ MHz.

Thus, $\tau_{op} \approx 6.25$ ns. We also take $\tau_{rot} \approx 1$ ns [20]. The criterion is whether all pulse sequences can be done during the dephasing time T_2. We will show that all generation times are less than 300 ns. Thus, if we assume $T_2 \sim 10$–20 μs with well-controlled pulses, which was realized by Paik *et al.* [43], we will be able to use the standard QECC process and correct qubit errors, as long as the number of errors is small.

III. GENERATION OF STABILIZER CODE FROM CONVENTIONAL HAMILTONIAN

Here, we show concrete pulse sequences to produce the target stabilizer Hamiltonians of the three major codes: the nine-qubit code, the five-qubit code, and the Steane code. In general, it is difficult to find a pulse sequence of the transformation from the conventional two-body solid-state Hamiltonian to the target stabilizer Hamiltonian, because the target Hamiltonians have Pauli matrices whose form is complicated. The best way to look for an appropriate pulse sequence is to change the target stabilizer Hamiltonian into a single-qubit Hamiltonian, because it is easier to reduce the number of multiplications of the Pauli matrices to a single-qubit Hamiltonian. In the following, we show the transformation process of H_{stab} of the three major codes to the initial single-qubit Hamiltonian. We also count the number of pulses and estimate the generation time of the codes. We show that the direct generation of H_{stab} is more effective than the previous method [20] in which G_i is generated one by one. The comparison of the present results with those of the previous results is summarized in Tables I and II.

A. Nine-qubit code

We would like to start from Shor's nine-qubit code, which was the first advanced QECC to be invented [1]. This code can correct single-qubit error ($n=9$, $k=1$), and the number of stabilizers is $l=8$. The stabilizers are given by $G_1 = Z_1Z_2$, $G_2 = Z_2Z_3$, $G_3 = Z_4Z_5$, $G_4 = Z_5Z_6$, $G_5 = Z_7Z_8$, $G_6 = Z_8Z_9$, $G_7 = X_1X_2X_3X_4X_5X_6$, and $G_8 = X_4X_5X_6X_7X_8X_9$ [3,4]. Then, the target stabilizer Hamiltonian is given by $H^{9code} = \sum_{i=1}^{8} G_i$ in which Ω_i are omitted, and we treat $H^{9code} = \sum_{i=1}^{8} G_i$ instead of $H^{9code} = -\sum_{i=1}^{8} G_i$ for clarity. We will treat the stabilizer Hamiltonians of the five-qubit code and the Steane code similarly. We consider how this target Hamiltonian is transformed to a single-qubit Hamiltonian by using Eqs. (15)–(17) for the XY interaction or Eqs. (20)–(22) for the Ising interaction. Let us first consider a case of the XY

TABLE I. The generation time of the stabilizer Hamiltonian of the XY interaction. "New generation time" is a generation time of the stabilizer Hamiltonian by using the proposed method. "Previous generation time" is a time, estimated by using the previous method [20]. $\tau_{op} = \pi/(4J)$. τ_{rot} represents a time of a single qubit rotation. We take $\tau_{op} = 6.25$ ns and $\tau_{rot} = 1$ ns (Sec. II E). "Improvement" is a ratio of reduction of time of the new generation, calculated from the third and fifth columns.

XY	Previous generation time		New generation time		Improvement
Nine-qubit code	$24\tau_{op} + 228\tau_{rot}$	378 ns	$16\tau_{op} + 92\tau_{rot}$	194 ns	48.7%
Five-qubit code	$24\tau_{op} + 162\tau_{rot}$	312 ns	$10\tau_{op} + 65\tau_{rot}$	127.5 ns	59.1%
Steane code	$44\tau_{op} + 288\tau_{rot}$	563 ns	$20\tau_{op} + 132\tau_{rot}$	257 ns	54.4%

TABLE II. The generation time of the stabilizer Hamiltonian from the Ising model. Parameters are the same as those in Table I.

Ising	Previous generation time		New generation time		Improvement
Nine-qubit code	$8\tau_{op} + 80\tau_{rot}$	130 ns	$10\tau_{op} + 61\tau_{rot}$	125.5 ns	3.5%
Five-qubit code	$14\tau_{op} + 97\tau_{rot}$	184.5 ns	$12\tau_{op} + 76\tau_{rot}$	151 ns	18.2%
Steane code	$36\tau_{op} + 220\tau_{rot}$	445 ns	$20\tau_{op} + 124\tau_{rot}$	249 ns	44%

interaction. $H^{9\text{code}}$ is changed as follows:

$$
\begin{aligned}
H^{9\text{code}} &= Z_1Z_2 + Z_2Z_3 + Z_4Z_5 + Z_5Z_6 + Z_7Z_8 + Z_8Z_9 + X_1X_2X_3X_4X_5X_6 + X_4X_5X_6X_7X_8X_9, \quad : (x \leftrightarrow z : 2,4,6,8), \\
&\to Z_1X_2 + X_2Z_3 + X_4Z_5 + Z_5X_6 + Z_7X_8 + X_8Z_9 - X_1Z_2X_3Z_4X_5Z_6 - Z_4X_5Z_6X_7Z_8X_9, \\
&\hspace{6cm} : H_{XY}^{12} + H_{XY}^{34} + H_{XY}^{56} + H_{XY}^{78}, \\
&\to -Y_1 - Y_1Z_2Z_4 - Y_3Z_4Z_6 - Y_5 - Y_7 - Y_7Z_8Z_9 + Y_2Y_4Y_6 - Z_3Y_6Y_8X_9, \quad : (y \leftrightarrow z : 1,5,7)(x \leftrightarrow z : 9) \\
&\to -Z_1 - Z_1Z_2Z_4 + Y_3Z_4Z_6 - Z_5 - Z_7 - Z_7Z_8X_9 + Y_2Y_4Y_6 + Z_3Y_6Y_8Z_9, \quad : H_{XY}^{34} + H_{XY}^{56} + H_{XY}^{89} \\
&\to -Z_1 - Z_1Z_2Z_3 + X_4Z_5 - Z_6 - Z_7 + Z_7Y_8 + Y_2X_3Z_4X_5Z_6 + Z_4X_5Z_6X_9, \quad : (x \leftrightarrow z : 3,4,5,9) \\
&\to -Z_1 - Z_1Z_2X_3 - Z_4X_5 - Z_6 - Z_7 + Z_7Y_8 + Y_2Z_3X_4Z_5Z_6 + X_4Z_5Z_6Z_9, \quad : H_{XY}^{23} + H_{XY}^{45} + H_{XY}^{78} \\
&\to -Z_1 + Z_1Y_2 + Y_4 - Z_6 - Z_8 + X_7 - X_3Y_5Z_6 - Y_5Z_6Z_9, \quad : (y \leftrightarrow z : 4)(x \leftrightarrow z : 7), H_{XY}^{12} + H_{XY}^{56} + H_{XY}^{89} \\
&\to -Z_2 + X_1 + Z_4 - Z_5 - Z_9 - Z_7 - X_3X_6 - X_6Z_8, \quad : (x \leftrightarrow z : 1,3) \\
&\to -Z_2 - Z_1 + Z_4 - Z_5 - Z_9 - Z_7 + Z_3X_6 - X_6Z_8, \quad : H_{XY}^{34} + H_{XY}^{78} \\
&\to -Z_2 - Z_1 + Z_3 - Z_5 - Z_9 - Z_8 + Z_4X_6 - X_6Z_7, \quad : H_{XY}^{45} + H_{XY}^{67} \\
&\to -Z_2 - Z_1 + Z_3 - Z_4 - Z_9 - Z_8 - Z_5Z_6Y_7 + Y_7, \quad : (x \leftrightarrow z : 5)(y \leftrightarrow z : 7) \\
&\to -Z_2 - Z_1 + Z_3 - Z_4 - Z_9 - Z_8 - X_5Z_6Z_7 + Z_7, \quad : H_{XY}^{56} \\
&\to -Z_2 - Z_1 + Z_3 - Z_4 - Z_9 - Z_8 + Y_6Z_7 + Z_7, \quad : H_{XY}^{67} \\
&\to -Z_2 - Z_1 + Z_3 - Z_4 - Z_9 - Z_8 + X_7 + Z_6.
\end{aligned}
\tag{34}
$$

Applied pulses are shown after the colon in each line. The notation $H_{XY}^{ij} = J_{ij}[X_iX_j + Y_iY_j]$ [Eq. (9)] on the right-hand side of each line after the colon shows that we apply Eq. (11) with $H_{op} = H_{XY}^{ij}$ to the Hamiltonian before the colon. For example, the second line of the above equation means that

$$
e^{i(\pi/4)[H_{XY}^{12}+H_{XY}^{34}+H_{XY}^{56}+H_{XY}^{78}]} H^{9\text{code}} e^{-i(\pi/4)[H_{XY}^{12}+H_{XY}^{34}+H_{XY}^{56}+H_{XY}^{78}]}.
\tag{35}
$$

The notation such as $(y \leftrightarrow z : 1,5,7,9)$ shows that single-qubit π rotation is applied to qubits 1, 5, 7, and 9 around the x axis. Thus when we start an initial Hamiltonian given by

$$
H_{\text{ini}}^{9\text{code}} = \Omega_1X_1 + \Omega_2X_2 + \Omega_3X_3 + \Omega_4X_4 + \Omega_6X_6 + \Omega_7X_7 + \Omega_8X_8 + \Omega_9X_9,
\tag{36}
$$

we can produce the stabilizer Hamiltonian $H^{9\text{code}}$ by using the pulse sequence described by the reverse operations of Eq. (34). The initial Hamiltonian, Eq. (36), is obtained by $e^{-itH_0}e^{i\pi X_5/2}e^{-itH_0}e^{-i\pi X_5/2}$ in which the e^{-itH_0} term is obtained from H_q as shown in the previous section. For the Ising interaction, we obtain

$$
\begin{aligned}
H^{9\text{code}} &\to X_1Z_2 + Z_2Z_3 + X_4Z_5 + Z_5Z_6 + Z_7Z_8 + Z_8X_9 - Z_1X_2X_3Z_4X_5Z_6 - Z_4X_5Z_6X_7X_8Z_9, \\
&\hspace{5cm} : H_{\text{Ising}}^{12} + H_{\text{Ising}}^{56} + H_{\text{Ising}}^{89} \\
&\to Y_1 + Z_2Z_3 + X_4Z_5 + Y_6 + Z_7Z_8 + Y_9 - Y_2X_3Z_4Y_5 - Z_4Y_5X_7Y_8, \quad : (y \leftrightarrow z : 2,8) \\
&\to Y_1 - Y_2Z_3 + X_4Z_5 + Y_6 - Z_7Y_8 + Y_9 - Z_2X_3Z_4Y_5 - Z_4Y_5X_7Z_8, \quad : H_{\text{Ising}}^{23} + H_{\text{Ising}}^{45} + H_{\text{Ising}}^{78} \\
&\to Y_1 + X_2 + Y_4 + Y_6 + X_8 + Y_9 + Y_3X_5 + X_5Y_7, \quad : H_{\text{Ising}}^{34} + H_{\text{Ising}}^{67} \\
&\to Y_1 + X_2 - Z_3X_4 - X_6Z_7 + X_8 + Y_9 - X_3Z_4X_5 - X_5Z_6X_7, \quad : (x \leftrightarrow z : 3,4,5,6,7) \\
&\to Y_1 + X_2 + X_3Z_4 + Z_6X_7 + X_8 + Y_9 - Z_3X_4Z_5 - Z_5X_6Z_7, \quad : H_{\text{Ising}}^{45} + H_{\text{Ising}}^{67} \\
&\to Y_1 + X_2 + X_3Z_4 + Y_7 + X_8 + Y_9 - Z_3Y_4 - Z_5Y_6, \quad : H_{\text{Ising}}^{34} + H_{\text{Ising}}^{56} \\
&\to Y_1 + X_2 + Y_3 + Y_7 + X_8 + Y_9 + X_4 + X_6,
\end{aligned}
\tag{37}
$$

where the notation $H_{\text{Ising}}^{ij} = J_{ij} Z_i Z_j$ [Eq. (10)] on the right-hand side of each line after the colon shows that we apply Eq. (11) with $H_{\text{op}} = H_{\text{Ising}}^{ij}$ to the Hamiltonian before the colon. After single-qubit rotations, we obtain an initial Hamiltonian:

$$H_{\text{ini}}^{9\text{code}} = \Omega_1 X_1 + \Omega_2 X_2 + \Omega_3 X_3 + \Omega_4 X_4$$
$$+ \Omega_6 X_6 + \Omega_7 X_7 + \Omega_8 X_8 + \Omega_9 X_9. \quad (38)$$

This Hamiltonian is obtained by eliminating the X_5 term in H_0 as in the case of the XY interaction.

Let us count the number of pulses necessary to obtain the nine-qubit code. Because the present method mainly relies on the control of many pulses, as the number of pulses increases, pulse errors become the principal origin of decoherence. Thus, the number of pulses is an indicator of decoherence in which it is desirable to have fewer pulses. Equation (36) shows that eight qubit-qubit interaction processes and five single-qubit rotation processes are needed. Because a time τ_{op} of applying Eq. (11) to H_{int}^{ij} is longer than a single-qubit rotation time τ_{rot} such as $\tau_{\text{op}}(\approx 6.25 \text{ ns}) > \tau_{\text{rot}}(\approx 1 \text{ ns})$ (see Sec. II E), the sixth operations of Eq. (34) can be represented by τ_{rot}. From the result of Sec. II D, it takes a time of $N_{\text{op}}[2\tau_{\text{op}} + 9\tau_{\text{rot}}]$ for N_{op} times uses of H_{XY}^{ij}, and the initial state Eq. (36) is obtained by twice using the generating process of H_0 taking a time of $10\tau_{\text{rot}}$. Thus, we need a time of

$$\tau_{XY}^{9\text{code(new)}} = 8[2\tau_{\text{op}} + 9\tau_{\text{rot}}] + 12\tau_{\text{rot}} + 10\tau_{\text{rot}}$$
$$= 16\tau_{\text{op}} + 94\tau_{\text{rot}}. \quad (39)$$

In order to compare the present method with that of Ref. [20], let us consider constructing H_{stab} of the XY interaction by summing up G_i as in Ref. [20]. For $G_1 \sim G_6$, it takes a time of $[2\tau_{\text{op}} + 9\tau_{\text{rot}}] + (4 + 10)\tau_{\text{rot}} = 2\tau_{\text{op}} + 23\tau_{\text{rot}}$, because $G_i \rightarrow Z_i X_{i+1} \rightarrow Y_i \rightarrow X_i$. For G_7, we have

$$G_7 = X_1 X_2 X_3 X_4 X_5 X_6, \quad : (x \leftrightarrow z : 2,5)$$
$$\rightarrow X_1 Z_2 X_3 X_4 Z_5 X_6, \quad : H_{XY}^{12} + H_{XY}^{56}$$
$$\rightarrow Y_2 X_3 X_4 Y_5, \quad : (x \leftrightarrow z : 3,4)$$
$$\rightarrow Y_2 Z_3 Z_4 Y_5, \quad : H_{XY}^{23} + H_{XY}^{45}$$

$$\rightarrow X_3 X_4, \quad : (x \leftrightarrow z : 3)$$
$$\rightarrow -Z_3 X_4, \quad : H_{XY}^{34}$$
$$\rightarrow Y_3, \quad : (y \leftrightarrow x : 3)$$
$$\rightarrow X_3. \quad (40)$$

Thus, it takes a time of $3[2\tau_{\text{op}} + 9\tau_{\text{rot}}] + 8\tau_{\text{rot}} + 10\tau_{\text{rot}} = 6\tau_{\text{op}} + 45\tau_{\text{rot}}$ to obtain G_7 and G_8. Thus, total generation time for the nine-qubit code by the method of Ref. [20] is given by $\tau_{XY}^{9\text{code(old)}} = 24\tau_{\text{op}} + 228\tau_{\text{rot}}$. Thus, the number of the qubit-qubit interaction of the present method is reduced to two-thirds of that of the previous method and the number of the single-qubit rotations is reduced to 41.2% of that of the previous method. When we use the experimental values in Sec. II E, $\tau_{XY}^{9\text{code(new)}} = 194$ ns and $\tau_{XY}^{9\text{code(old)}} = 376$ ns, thus 48.7% reduction of the operation time is achieved. For the Ising interaction, from Eq. (37), we obtain a time of the operation given by

$$\tau_{\text{Ising}}^{9\text{code(new)}} = 10\tau_{\text{op}} + 63\tau_{\text{rot}} = 125.5 \text{ ns}. \quad (41)$$

Here, we used the experimental value of $\tau_{\text{op}} \approx 6.25$ ns and $\tau_{\text{rot}} \approx 1$ ns (see Sec. II E). $G_1 \sim G_6$ have the form of the two-body interaction, thus they are directly extracted from H_q as shown in Sec. II D. Thus it takes a time of $4\tau_{\text{rot}}$ for each process. G_7 and G_8 are reduced to $Z_3 Z_4$ and $Z_6 Z_7$ with a time of $4\tau_{\text{op}} + 28\tau_{\text{rot}}$, respectively. Therefore, we obtain $\tau_{\text{Ising}}^{9\text{code(old)}} = 8\tau_{\text{op}} + 80\tau_{\text{rot}} = 130$ ns. For this case, a 3.5% reduction of time is achieved.

B. Five-qubit code

Next, we consider H_{stab} of the five-qubit code ($n = 5$ and $k = 1$). The stabilizers G_i ($i = 1, \ldots, 4$) of this code are given by $G_1 = X_1 Z_2 Z_3 X_4$, $G_2 = X_2 Z_3 Z_4 X_5$, $G_3 = X_3 Z_4 Z_5 X_1$, and $G_4 = X_4 Z_5 Z_1 X_2$ [3,4]. The process of constructing $H^{5\text{code}} \equiv \sum_{i=1}^{4} G_i$ is obtained by changing the $H^{5\text{code}}$ reversely into a single-qubit Hamiltonian. For the XY model, this process is obtained by

$$H^{5\text{code}} = X_1 Z_2 Z_3 X_4 + X_2 Z_3 Z_4 X_5 + X_3 Z_4 Z_5 X_1 + X_4 Z_5 Z_1 X_2, \quad : H_{XY}^{12} + H_{XY}^{34}$$
$$\rightarrow Y_2 Y_3 - Y_1 Z_2 Z_3 Z_4 X_5 + Y_4 Z_5 Z_1 Y_2 + Y_3 Z_4 Z_5 Y_1, \quad : (y \leftrightarrow z : 2)$$
$$\rightarrow Z_2 Y_3 + Y_1 Y_2 Z_3 Z_4 X_5 + Y_4 Z_5 Z_1 Z_2 + Y_3 Z_4 Z_5 Y_1, \quad : H_{XY}^{23} + H_{XY}^{45}$$
$$\rightarrow X_2 - Y_1 X_3 Y_4 + Z_1 Z_3 X_5 + Y_1 X_2 Z_3 Z_4 Z_5, \quad : (x \leftrightarrow z : 2,3)$$
$$\rightarrow -Z_2 + Y_1 Z_3 Y_4 + Z_1 X_3 X_5 - Y_1 Z_2 X_3 Z_4 Z_5, \quad : H_{XY}^{12} + H_{XY}^{34}$$
$$\rightarrow -Z_1 + Z_1 X_2 X_3 - Z_2 Z_3 Y_4 X_5 + X_2 Y_4 Z_5, \quad : (x \leftrightarrow z : 2)(y \leftrightarrow z : 4,5)$$
$$\rightarrow -Z_1 - Z_1 Z_2 X_3 - X_2 Z_3 Z_4 X_5 + Z_2 Z_4 Y_5, \quad : H_{XY}^{23} + H_{XY}^{45}$$
$$\rightarrow -Z_1 + Z_1 Y_2 - Y_3 Y_4 + Z_3 X_4, \quad : (y \leftrightarrow z : 4)$$
$$\rightarrow -Z_1 + Z_1 Y_2 - Y_3 Z_4 + Z_3 X_4, \quad : H_{XY}^{12} + H_{XY}^{34}$$
$$\rightarrow -Z_2 + X_1 - X_4 - Y_3. \quad (42)$$

The notations are the same as those in Eq. (34) such that the applied pulses are shown after the colon in each line. The two-body XY interaction $H_{XY}^{ij} = J_{ij}[X_i X_j + Y_i Y_j]$ on the right-hand side of each line after the colon shows that we apply Eq. (11) to the

Hamiltonian before the colon by using Eqs. (15)–(17). Then, the initial Hamiltonian is given by

$$H_{\text{ini}}^{\text{5code}} = \Omega_1 X_1 + \Omega_2 X_2 + \Omega_3 X_3 + \Omega_4 X_4. \tag{43}$$

The time of constructing this code is given by

$$\tau_{XY}^{\text{5code(new)}} = 5[2\tau_{\text{op}} + 9\tau_{\text{rot}}] + 10\tau_{\text{rot}} + 10\tau_{\text{rot}} = 10\tau_{\text{op}} + 65\tau_{\text{rot}} = 127.5 \text{ ns}. \tag{44}$$

If we use the previous method in Ref. [20], we have $\tau_{XY}^{\text{5code(old)}} = 24\tau_{\text{op}} + 162\tau_{\text{rot}} = 312$ ns. This result is a little different from that in Ref. [20] in that here we start from 2D Hamiltonian. Thus, a 59.1% reduction of time is expected with the present method. For the Ising interaction, we have

$$
\begin{aligned}
H^{\text{5code}} &\to Z_1 X_2 X_3 Z_4 + Z_2 X_3 X_4 Z_5 + Z_1 Z_3 X_4 X_5 + X_1 Z_2 Z_4 X_5, \ : H_{\text{Ising}}^{23} \\
&\to Z_1 X_2 X_3 Z_4 + Y_3 X_4 Z_5 + Z_1 Z_3 X_4 X_5 + X_1 Z_2 Z_4 X_5, \ : (x \leftrightarrow z : 1,2)(y \leftrightarrow z : 3) \\
&\to -X_1 Z_2 X_3 Z_4 + Z_3 X_4 Z_5 - X_1 Y_3 X_4 X_5 - Z_1 X_2 Z_4 X_5, \ : H_{\text{Ising}}^{12} + H_{\text{Ising}}^{34} \\
&\to -Y_1 Y_3 + Y_4 Z_5 - Y_1 Z_2 Y_3 X_4 X_5 - Y_2 Z_4 X_5, \ : (y \leftrightarrow z : 1,2,4)(x \leftrightarrow z : 5) \\
&\to -Z_1 Y_3 + Z_4 X_5 - Z_1 Y_2 Y_3 X_4 X_5 - Z_2 Y_4 X_5, \ : H_{\text{Ising}}^{12} + H_{\text{Ising}}^{45} \\
&\to -Z_1 Y_3 + Y_5 + X_2 Y_3 Y_4 + Z_2 X_4, \ : (x \leftrightarrow z : 2) \\
&\to -Z_1 Y_3 + Y_5 - Z_2 Y_3 Y_4 + X_2 X_4, \ : H_{\text{Ising}}^{23} \\
&\to Z_1 Z_2 X_3 + Y_5 + X_3 X_4 + Y_2 Z_3 X_4, \ : (y \leftrightarrow z : 2)(x \leftrightarrow z : 3,4) \\
&\to Z_1 Y_2 Z_3 + Y_5 - Z_3 Y_4 - Z_2 X_3 Z_4, \ : H_{\text{Ising}}^{23} \\
&\to -Z_1 X_2 + Y_5 - Z_3 Y_4 - Y_3 Z_4, \ : H_{\text{Ising}}^{12} + H_{\text{Ising}}^{34} \\
&\to -Y_2 + Y_5 + X_4 + X_3,
\end{aligned}
\tag{45}
$$

where the Ising interaction $H_{\text{Ising}}^{ij} = J_{ij} Z_i Z_j$ on the right-hand side of each line shows that we apply Eqs. (20)–(22) based on Eq. (11) with $H_{\text{op}} = H_{\text{Ising}}^{ij}$. Thus, the initial Hamiltonian from which H_{stab} is derived is given by

$$H_{\text{ini}}^{\text{5code}} = \Omega_2 X_2 + \Omega_3 X_3 + \Omega_4 X_4 + \Omega_5 X_5. \tag{46}$$

The time for the generation of this code is $6[2\tau_{\text{op}} + 9\tau_{\text{rot}}] + 12\tau_{\text{rot}} + 10\tau_{\text{rot}} = 151$ ns. Because $G_1 = X_1 Z_2 Z_3 X_4 \to Z_1 X_2 X_3 Z_4 \to Y_2 Y_3 \to Z_2 Z_3$, it takes a time of $[2\tau_{\text{op}} + 9\tau_{\text{rot}}] + 4\tau_{\text{rot}} + 4\tau_{\text{rot}} = 2\tau_{\text{op}} + 17\tau_{\text{rot}}$ to obtain G_1 and G_2. G_3 is estimated from

$$
\begin{aligned}
G_3 &= X_1 X_3 Z_4 Z_5, \ : (x \leftrightarrow z : 1,4) \\
&\to -Z_1 X_3 X_4 Z_5, \ : H_{XY}^{23} + H_{XY}^{45} \\
&\to -Z_1 Z_2 Y_3 Y_4, \ : (y \leftrightarrow z : 2,4) \\
&\to Z_1 Y_2 Y_3 Z_4, \ : H_{XY}^{12} + H_{XY}^{34}
\end{aligned}
$$

$$
\begin{aligned}
&\to X_2 X_3, \ : (x \leftrightarrow z : 2,3) \\
&\to Z_2 Z_3.
\end{aligned}
\tag{47}
$$

Thus it takes $4\tau_{\text{op}} + 28\tau_{\text{rot}}$. Similarly, it takes $6\tau_{\text{op}} + 35\tau_{\text{rot}}$ for G_4. Therefore, in total, it takes $14\tau_{\text{op}} + 97\tau_{\text{rot}} = 184.5$ ns for summing up $G_1 \sim G_4$ in the Ising interaction. In this case the present method reduces the generation time by 18.2%.

C. Steane code

The stabilizers of the Steane code are described by $G_1 = X_1 X_2 X_3 X_4$, $G_2 = X_1 X_2 X_5 X_6$, $G_3 = X_1 X_3 X_5 X_7$, $G_4 = Z_1 Z_2 Z_3 Z_4$, $G_5 = Z_1 Z_2 Z_5 Z_6$, and $G_6 = Z_1 Z_3 Z_5 Z_7$ [3,4]. Because G_4, G_5, and G_7 are obtained from G_1, G_2, and G_3 by applying π pulses, we first consider the generation process of $H_X^{\text{Steane}} \equiv G_1 + G_2 + G_3$. The process of the construction of H_X^{Steane} is obtained by resolving it to a single-qubit Hamiltonian. For the case of the XY Hamiltonian, this process is given by

$$
\begin{aligned}
H_X^{\text{Steane}} &= X_1 X_2 X_3 X_4 + X_1 X_2 X_5 X_6 + X_1 X_3 X_5 X_7, \ : (x \leftrightarrow z : 2,3,5) \\
&\to X_1 Z_2 Z_3 X_4 + X_1 Z_2 Z_5 X_6 + X_1 Z_3 Z_5 X_7, \ : H_{XY}^{12} + H_{XY}^{34} + H_{XY}^{56} \\
&\to Y_2 Y_3 + Y_2 Y_5 - Z_1 Y_2 Z_4 Z_6 X_7, \ : (y \leftrightarrow z : 2,5) \\
&\to Z_2 Y_3 + Z_2 Z_5 - Z_1 Z_2 Z_4 Z_6 X_7, \ : H_{XY}^{23} + H_{XY}^{45} + H_{XY}^{67} \\
&\to X_2 + Z_3 Z_4 + Z_1 Z_3 Z_5 Y_6, \ : (x \leftrightarrow z : 2,4) \\
&\to -Z_2 + Z_3 X_4 + Z_1 Z_3 Z_5 Y_6, \ : H_{XY}^{12} + H_{XY}^{34} + H_{XY}^{56} \\
&\to -Z_1 - Y_3 + Z_2 Z_4 X_5, \ : (y \leftrightarrow z : 3) \\
&\to -Z_1 - Z_3 + Z_2 Z_4 X_5, \ : H_{XY}^{23} + H_{XY}^{45}
\end{aligned}
$$

$$\rightarrow -Z_1 - Z_2 - Z_3 Y_4, \ : H_{XY}^{34}$$
$$\rightarrow -Z_1 - Z_2 - X_3, \tag{48}$$

where the notations are the same as those in Eqs. (34) and (42). Thus, we obtain the initial Hamiltonian:

$$H_{X:\text{ini}}^{\text{Steane}} = \Omega_1 X_1 + \Omega_2 X_2 + \Omega_3 X_3. \tag{49}$$

The time of generation of H_X^{Steane} is the same as Eq. (44). For the previous method, the time for obtaining H_X^{Steane} is given by $22\tau_{\text{op}} + 143\tau_{\text{rot}}$. As mentioned above, because $H_Z^{\text{Steane}} \equiv G_4 + G_5 + G_6$ is obtained by

$$H_Z^{\text{Steane}} = e^{-i\pi(Y_1+Y_2+Y_3)/4} H_X^{\text{Steane}} e^{i\pi(Y_1+Y_2+Y_3)/4}, \tag{50}$$

the generation time of H_Z^{Steane} is increased by $2\tau_{\text{rot}}$ compared with that of H_X^{Steane}. Then, the time of obtaining the Steane code by the present method is given by

$$\tau_{XY}^{\text{Steane(new)}} = 20\tau_{\text{op}} + 132\tau_{\text{rot}} = 257 \text{ ns}. \tag{51}$$

When we use the previous method in Ref. [20], the time for the code generation is given by $\tau_{XY}^{\text{Steane(old)}} = 44\tau_{\text{op}} + 288\tau_{\text{rot}} = 563$ ns. Thus, a 54.4% reduction of time is expected.

For the Ising Hamiltonian, we have

$$\begin{aligned}
H_X^{\text{Steane}} &= X_1 X_2 X_3 X_4 + X_1 X_2 X_5 X_6 + X_1 X_3 X_5 X_7, \ : (z \leftrightarrow x : 1,4,6) \\
&\rightarrow Z_1 X_2 X_3 Z_4 + Z_1 X_2 X_5 Z_6 - Z_1 X_3 X_5 X_7, \ : H_{\text{Ising}}^{12} + H_{\text{Ising}}^{34} + H_{\text{Ising}}^{56} \\
&\rightarrow Y_2 Y_3 + Y_2 Y_5 - Z_1 Y_3 Z_4 Y_5 Z_6 X_7, \ : (y \leftrightarrow z : 3)(x \leftrightarrow z : 6,7) \\
&\rightarrow Y_2 Z_3 + Y_2 Y_5 + Z_1 Z_3 Z_4 Y_5 X_6 Z_7, \ : H_{\text{Ising}}^{23} + H_{\text{Ising}}^{45} + H_{\text{Ising}}^{67} \\
&\rightarrow -X_2 + X_2 Z_3 Z_4 X_5 - Z_1 Z_3 X_5 Y_6, \ : (x \leftrightarrow z : 2,3,4,5) \\
&\rightarrow Z_2 + Z_2 X_3 X_4 Z_5 + Z_1 X_3 Z_5 Y_6, \ : H_{\text{Ising}}^{23} + H_{\text{Ising}}^{45} \\
&\rightarrow Z_2 + Y_3 Y_4 + Z_1 Z_2 Y_3 Z_5 Y_6, \ : (y \leftrightarrow z : 2,4,5,6) \\
&\rightarrow -Y_2 + Y_3 Z_4 + Z_1 Y_2 Y_3 Y_5 Z_6, \ : H_{\text{Ising}}^{12} + H_{\text{Ising}}^{34} + H_{\text{Ising}}^{56} \\
&\rightarrow Z_1 X_2 - X_3 - X_2 X_3 Z_4 X_5, \ : (x \leftrightarrow z : 2,4,5) \\
&\rightarrow -Z_1 Z_2 - X_3 - Z_2 X_3 X_4 Z_5, \ : H_{\text{Ising}}^{23} + H_{\text{Ising}}^{45} \\
&\rightarrow -Z_1 Z_2 - Z_2 Y_3 - Y_3 Y_4, \tag{52}
\end{aligned}$$

where the notations are the same as those in Eqs. (37) and (45). Thus, the initial Hamiltonian is given by

$$H_{X:\text{ini}}^{\text{Steane}} = J_{12} Z_1 Z_2 + J_{23} Z_2 Z_3 + J_{34} Z_3 Z_4. \tag{53}$$

This Hamiltonian is obtained by erasing H_{Ising}^{45} from H_{Ising} where H_{Ising} is obtained by applying π pulses to all qubits in B of Eq. (23). Then, Eq. (53) is obtained by applying a π pulse only to qubit 5 in B of Eq. (23) for H_{Ising}, and the time of the preparation of Eq. (53) is estimated by $4\tau_{\text{rot}}$. Therefore, the total time of the generation of Eq. (52) is given by $5[2\tau_{\text{op}} + 9\tau_{\text{rot}}] + 12\tau_{\text{rot}} + 4\tau_{\text{rot}} = 123.5$ ns, and $\tau_{\text{Ising}}^{\text{Steane(new)}} = 20\tau_{\text{op}} + 124\tau_{\text{rot}} = 249$ ns. On the other hand, in the previous method, times for generating G_1, G_2, and G_3 are given by $4\tau_{\text{op}} + 26\tau_{\text{rot}}$, $6\tau_{\text{op}} + 35\tau_{\text{rot}}$, and $8\tau_{\text{op}} + 48\tau_{\text{rot}}$, respectively. Therefore, $\tau_{\text{Ising}}^{\text{Steane(old)}} = 36\tau_{\text{op}} + 220\tau_{\text{rot}} = 445$ ns. This means that the present method realizes a 44% reduction of time.

All the results of the above-mentioned three codes are summarized in Tables I and II for the XY interaction and Ising interaction, respectively. From Tables I and II, we can see the large reduction of the generation time is achieved in the XY interaction.

IV. CREATION OF THE STANDARD CODES

As briefly reviewed in Sec. II A, encoded states are generated by repeating measurements of the stabilizers G_i ($i = 1, \ldots, l$) for an initial state $\Pi_{i=1}^k |0\rangle_n$ [3,4]. Considering that measurements induce extra decoherence, the effectiveness of this conventional method is limited. In Ref. [20], we presented the more effective method of directly generating logical states: For any given code, only those G_j with $1 \leqslant j \leqslant m$ and $m \leqslant n - k$ that contain X or Y operators are needed for the preparation:

$$\begin{aligned}
|\bar{c}_1, \ldots, \bar{c}_k\rangle &= (1 + G_1) \cdots (1 + G_m) \bar{X}_1^{c_1} \cdots \bar{X}_k^{c_k} |0, \ldots, 0\rangle \\
&= \prod_{i=1}^k \bar{X}_i^{c_i} \prod_{j=1}^m \exp\left(-i \frac{\pi}{4} \tilde{G}_j^{a_j} \right) |0, \ldots, 0\rangle, \tag{54}
\end{aligned}$$

where $c_i = 0, 1$ and operators $\bar{X}_i$ act in the logical state space $\{|\bar{0}\rangle_i, |\bar{1}\rangle_i\}$. Here, $\tilde{G}_j^{a_j}$ denotes a modified stabilizer operator obtained from G_j by replacing the X operator acting on qubit a_j by a Y operator, or vice versa. This is done in order to match the effect of an *individual* factor $\exp[i(\pi/4)\tilde{G}_j^{a_j}]$ with the action of the projector $(1 + G_j)$ when qubit a_j is in state $|0\rangle$. To fulfill Eq. (54) for all $1 \leqslant j \leqslant m$ *simultaneously*, all the a_j have to be different and the modified stabilizers have to

be generated in an order such that prior to $\tilde{G}_j^{a_j}$ none of the $\tilde{G}_k^{a_k}$ with $k < j$ have acted on qubit a_j with an X or Y. The time for generating the encoded state is given by $\tau_{\text{stab}} + (\sum_i c_i)\tau_{\text{rot}}$.

Here, we extend this idea further and consider whether we can replace this equation by

$$|\bar{0}\rangle = \exp\left(-i\frac{\pi}{4}\tilde{H}_{\text{stab}}\right)|0\rangle, \tag{55}$$

$$\tilde{H}_{\text{stab}} \equiv \sum_i \tilde{G}_i. \tag{56}$$

For the five-qubit code, we need $\tilde{G}_1 = Y_1 Z_2 Z_3 X_4$, $\tilde{G}_2 = X_2 Z_3 Z_4 Y_5$, $\tilde{G}_3 = X_1 Y_3 Z_4 Z_5$, and $\tilde{G}_4 = Z_1 Y_2 X_4 Z_5$, and the multiplication is carried out in the following order: $\exp[i(\pi/4)\tilde{G}_2]$, $\exp[i(\pi/4)\tilde{G}_4]$, $\exp[i(\pi/4)\tilde{G}_3]$, $\exp[i(\pi/4)\tilde{G}_1]$. However, only $\tilde{G}_3$ and $\tilde{G}_4$ commute, thus we cannot replace Eq. (54) by Eq. (56).

For the Steane code, we need three generators:

$$\tilde{G}_1 = X_1 X_2 X_3 Y_4, \tag{57}$$

$$\tilde{G}_2 = X_1 X_2 X_5 Y_6, \tag{58}$$

$$\tilde{G}_3 = X_1 X_3 X_5 Y_7, \tag{59}$$

because these three generators mutually commute, such as $[\tilde{G}_i, \tilde{G}_j] = 0$. Therefore we can apply Eq. (56) and reduce the generation time of the encoded state. Thus, it is observed that sparse distribution of the Pauli operators in a logical qubit is preferable for the code generation, because it results in simpler generation of encoded states.

Next, we consider an encoding of unknown state $a|0\rangle + b|1\rangle$ to $a|\bar{0}\rangle + b|\bar{1}\rangle$ (a and b are arbitrary complex numbers). Because, in Eq. (54), $\tilde{G}_j^{a_j}$ was introduced to hold $\exp[-i(\pi/4)\tilde{G}_j^{a_j}]|0\rangle = (1 + G_j)|0\rangle$, we need different operations for obtaining $|\bar{1}\rangle$. For simplicity, we consider $|\bar{1}\rangle = \bar{X}|\bar{0}\rangle$. Then, we can solve this problem if we can prepare a modified initial state for $|1\rangle$ defined by

$$|\bar{1}\rangle' = \bar{M}^{-1}\bar{X}\bar{M}|0,\ldots,0\rangle, \tag{60}$$

with $\bar{M} \equiv \prod_{j=1}^m \exp[-i(\pi/4)\tilde{G}_j^{a_j}]$. This is because we can use the following relation:

$$\bar{M}(a|0,\ldots,0\rangle + b|\bar{1}\rangle') = a|\bar{0}\rangle + b|\bar{1}\rangle. \tag{61}$$

For the five-qubit code, $\bar{X}$ is given by $\bar{X} = X_1 X_2 X_3 X_4 X_5$ [3], and the modified initial state $|\bar{1}\rangle'$ is expressed by $|\bar{1}\rangle' = -\tilde{G}_3 \tilde{G}_2 \bar{X}|00000\rangle = -|00010\rangle$. This means that we can obtain an encoded unknown state $a|\bar{0}\rangle + b|\bar{1}\rangle$ when we encode an initial unknown state $a|0\rangle + b|1\rangle$ into the fourth qubit described by $|0\rangle_1|0\rangle_2|0\rangle_3(a|0\rangle_4 - b|1\rangle_4)|0\rangle_5$ (the phase of $|1\rangle_4$ is changed). For the Steane code, $\bar{X}$ is given by $\bar{X} = X_5 X_6 X_7$ [3], and the modified initial state $|\bar{1}\rangle'$ is expressed by $|\bar{1}\rangle' = X_2 X_3 X_5|00000\rangle = |0110100\rangle$. Hence, we have to prepare $a|0000000\rangle + b|0110100\rangle$ to which $\bar{M}$ is applied. This state is transformed from $|0\rangle_1(a|0\rangle_2 + b|1\rangle_2)|00000\rangle$ by applying CNOT gates in which qubits 3 and 5 are target qubits, while qubit 2 is the control qubit.

The nine-qubit codes can be generated in a different way, because the nine-qubit code is expressed by the product of three parts given by [1]

$$|\bar{0}\rangle \equiv (|000\rangle + |111\rangle)(|000\rangle + |111\rangle)(|000\rangle + |111\rangle), \tag{62}$$

$$|\bar{1}\rangle \equiv (|000\rangle - |111\rangle)(|000\rangle - |111\rangle)(|000\rangle - |111\rangle). \tag{63}$$

Each three-qubit block is a Greenberger-Horne-Zeilinger (GHZ) state. From $|000\rangle \pm |111\rangle = \exp[\mp i(\pi/4)X_1 Y_2 X_3]|000\rangle$, we have

$$|\bar{0}\rangle = \exp\left(-i\frac{\pi}{4}H_0^{9\text{code}}\right)|0,\ldots,0\rangle, \tag{64}$$

$$|\bar{1}\rangle = \exp\left(i\frac{\pi}{4}H_0^{9\text{code}}\right)|0,\ldots,0\rangle, \tag{65}$$

where the Hamiltonian $H_0^{9\text{code}} \equiv X_1 Y_2 X_3 + X_4 Y_5 X_6 + X_7 Y_8 X_9$ is obtained starting from $X_1 + X_4 + X_7$ by applying operations discussed in the previous sections. The concrete pulse sequence is given by (1) $H_{XY}^{12} + H_{XY}^{45} + H_{XY}^{67}$, (2) $H_{XY}^{34} + H_{XY}^{56} + H_{XY}^{78}$, and (3) single-qubit rotations. Unknown state $a|0\rangle + b|1\rangle$ is encoded by applying $\exp(-i\frac{\pi}{4}H_0^{9\text{code}})$ to a changed state $a|0,\ldots,0\rangle + b|1,\ldots,1\rangle$ which can be obtained by CNOT gate to $(a|0\rangle + b|1\rangle)|0,\ldots,0\rangle$.

V. QUBIT ARCHITECTURE

Let us consider possible encoded qubit architectures for solid-state qubits controlled by local gate electrodes. In general, solid-state qubits are fabricated on some substrate and, unlike optical qubits and ion trap qubits [46], they cannot be moved, being subject to the restriction that the interactions between qubits are limited to the nearest qubits. Thus, as discussed in Sec. II D 2, it is natural to set a logical qubit as a 1D array. In order to construct various stabilizer codes, every qubit should be accessed by an appropriate gate electrode. This means that a gate electrode layer should be placed along logical qubits. Because logical qubits interact with each other in a 2D plane, the gate electrode layer will be constructed on or under the logical qubit layer.

Next, let us consider a structure of measurements. For the fault-tolerant computation, additional measurement circuits are required as described in Refs. [4,5]. Figure 2 shows the measurement circuit for a single-qubit measurement and the multiqubit measurement. The multiqubit measurement is used for stabilizer formalism [Fig. 2(b)]. In Fig. 2(b), the number of qubits in the cat state $|0,\ldots,0\rangle + |1,\ldots,1\rangle$, depends on the number of Pauli matrices of the stabilizer [Fig. 2(b) is the case of a three-qubit stabilizer]. This means that the number of ancilla qubits for the whole measurement circuit is of the same order as that of qubits in a logical qubit layer. Therefore, so as to avoid direct measurements and achieve the fault-tolerant computation, it is appropriate to set an independent qubit layer for measurements. Because we already have a logical qubit layer, it is natural that the additional measurement layer should be stacked as shown in Fig. 3. Note that physical qubits and electrodes in Fig. 3 are described in an abstract form. Real qubits and electrodes are more complicated than a box. Thus,
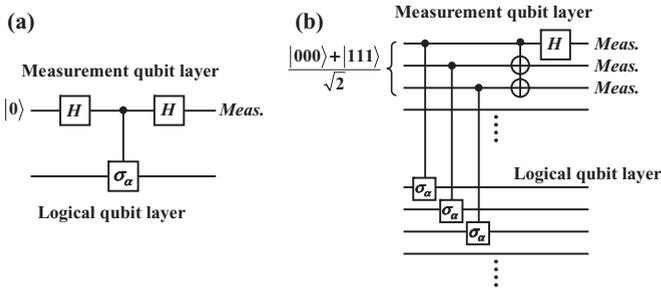
FIG. 2. Measurement circuit for fault-tolerant quantum computation [4]. In order to apply any kind of QECC, measurement qubit is required for every physical qubit in the logical qubit layer. (a) Single-qubit measurement. (b) Multiqubit measurement. H shows a Hadamard gate.

a stacked 3D qubit system will be straightforward architecture for an effective QECC system, as long as we assume that the interaction between physical qubits is restricted to their neighboring qubits. For generating the cat state of qubits in the measurement layer, our method shown in the previous section regarding the nine-qubit code generation is useful.

The stacked 3D qubit system can be applied to spin qubits and charge qubits. However, not all qubits can be stacked in the 3D system. Consider an example of standard superconducting flux qubits. If we stack flux qubits, the same flux penetrates stacked two qubits, resulting in confusion of signal between the stacked flux qubits. In such case, we will be able to implement a single logical qubit into a square form as shown in Fig. 4. The 2D arrangement consists of four logical qubits placed at the peripheral and ancilla qubits surrounded by the logical qubits. The four logical qubits share their quantum information through SWAP operation in the ancilla qubits and connect to the four directions of the nearest logical qubits. The ancilla qubits at the central region work for fault-tolerant measurements.

VI. ROBUSTNESS AGAINST PULSE ERRORS

Since the code word states are encoded in the twofold-degenerate ground-state manifold $|\bar{0}\rangle$ and $|\bar{1}\rangle$ of H_{stab}, the robustness of this method is limited by the rate of leakage out of this manifold. Thus, energy nonconserving single-qubit
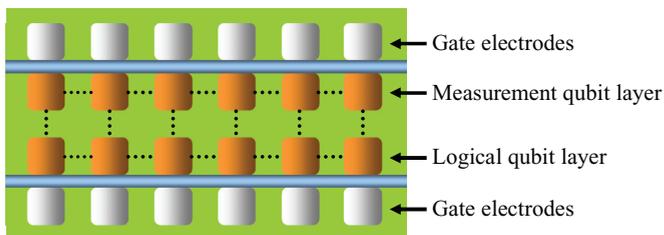

FIG. 3. (Color online) Layered 3D QECC system. There are two qubit layers; a logical qubit layer and a measurement qubit layer. Each qubit layer is connected to a gate electrode layer by which physical qubits are controlled. Boxes show qubits and electrodes. Dot lines show qubit-qubit interaction. In the stabilizer coded, measurement is an indispensable process for encoding and decoding. Thus, the logical qubit layer is set close to the measurement qubit layer.
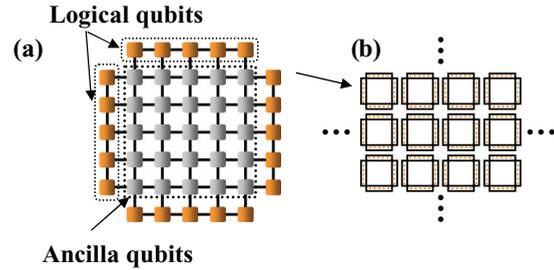

FIG. 4. (Color online) 2D qubit layout. Small box shows physical qubits. (a) Single logical qubit unit, which is composed of four peripheral logical qubits and central ancilla qubits. The four peripheral qubits are processed to be equivalent. They interact with logical qubits of other logical qubit units. (b) 3×4 logical qubit array where each square corresponds to the logical qubit of (a).

errors—often a prevalent kind of error created by a thermal bath—are exponentially suppressed for temperatures that are low compared to the Zeeman splitting Ω. Hence, besides local imperfections and noise sources, unavoidable pulse errors are likely to be the predominant cause of leakage, at low temperatures.

In the present method, each logical qubit is constructed by starting from a single-qubit Hamiltonian $\sum_i \Omega_i Z_i$, and multiplying operators like $X_1 \to X_1 X_2 \to X_1 \cdots X_N$. Hence, it is possible that this process makes operation errors transmit through each logical qubit. If we model the pulse errors by randomly distributed, unbiased, and uncorrelated deviations $\delta\theta$ with $\sigma_\theta = \sqrt{\langle \delta\theta^2 \rangle}$ from the ideal angle of $\pi/2$. The leakage from the twofold-degenerate ground-state manifold $|\bar{0}\rangle$ and $|\bar{1}\rangle$ can then be estimated by looking at the average of the ground-state fidelity $\langle F(t) \rangle \approx 1 - N_{\text{P}} \sigma_\theta^2 t / (8\mathcal{T})$, where N_{P} is the number of pulses in the sequence to generate H_{stab}, and $\mathcal{T}$ its duration [20]. Thus, the reduction of the number of pulses N_{P} for generating stabilizer codes (Tables I and II) is very important.

For the QECC scheme to succeed, the error rate of each qubit operation should be less than 10^{-7}–10^{-5} [4,5]. Thus the accuracy of operation pulses is crucial. In this regard, we can also use one of many NMR techniques. If we construct each single pulse by composite pulses, the accuracy of the pulse increases dramatically [21]. The composite-pulse method generalizes the concept of spin echo, and has already been applied in the field of quantum computation to greatly improve both single-qubit rotations and CNOT operations [22–25]. As the number of pulses N_{P} decreases and the dephasing time T_2 increases, more accurate composite pulses can be implemented, resulting in the success of the QECC scheme.

VII. SUMMARY AND CONCLUSIONS

In summary, we showed how to produce stabilizer Hamiltonians starting from natural two-body Hamiltonians by using appropriate pulse sequences. We demonstrated our method by using typical codes: the nine-qubit code, the five-qubit code, and the Steane code. The key method of finding the pulse sequence is to inversely trace the derivation process from the stabilizer Hamiltonian to the single-qubit Hamiltonian. We also showed how to generate encoded states without

using measurements. Stabilizer Hamiltonians are important for preserving encoded states as ground states of the system. Effective preparation of stabilizers is considered to be critical to the success of the QECC.

Many important experiments have been performed to enlarge coherence time in solid-state qubits [47]. The criteria for the realization of quantum computing is whether a sufficient number of quantum operations can be carried out during a given coherence time. Thus, manipulation speed of each quantum operation is one of the most important factors for practical quantum computing. Considering the fact that a quantum computer exceeds a digital computer only in several fields such as search algorithm, it will be natural to embed a quantum computer as a part of a digital computer system. Moreover, as in the present experiments, a quantum circuit will be operated by a digital computer. Although the speed of a single processing unit of a commercial digital computer seems to become saturated, performance of digital computers will continue to increase by parallel processing. Accordingly, it is expected that the manipulation speed of a pulse sequence will also increase. Therefore, the approach presented in this paper enables faster quantum operations by using the cutting-edge technology of computer science. How to achieve an appropriate and smooth connection between a quantum computer and a digital computer will be a future problem.

ACKNOWLEDGMENTS

APPENDIX A: EXTRACTION PARTS OF OTHER TYPES OF HAMILTONIANS

Here, we show how to extract H_0 or interaction parts from a Hamiltonian that includes three Pauli matrices X, Y, and Z. This situation appears for Eq. (6) with $\omega_i^{\mathrm{rf}} \neq 2\Omega_{0i}$ or Ref. [48] in which the Hamiltonian is given by

$$H = \sum_i [\omega_i Z_i + \epsilon_i X_i] + \sum_{i<j} \frac{J_{ij}}{2}[X_i X_j + Y_i Y_j]. \quad (A1)$$

For this Hamiltonian, one more step is required to obtain both H_0 and an interaction part. When the method of Sec. II D 3 is applied, we obtain $H_{\mathrm{eff}} = \sum_{k,i}[4\omega_i Z_i^{(k)} + 2\epsilon_i X_i^{(k)}]$ after using Eq. (24). When the method of Sec. II D 4 is applied, we obtain $H'_{\mathrm{eff}} = \sum_k[\sum_i 4Z_i^{(k)} + \sum_i H_{XY}^{23(k)}]$. In both cases, an extra $\sum_i Z_i$ term remains. Therefore, we need one more step to delete the $\sum_i Z_i$ term such as $e^{-i\tau H_{\mathrm{eff}}}e^{-i\pi \sum_i X_i/2}e^{-i\tau H_{\mathrm{eff}}}e^{i\pi \sum_i X_i/2}$ and $e^{-i\tau H'_{\mathrm{eff}}}e^{-i\pi \sum_i X_i/2}e^{-i\tau H'_{\mathrm{eff}}}e^{i\pi \sum_i X_i/2}$.

APPENDIX B: PERTURBATION TERMS IN BCH FORMULA

Here, we show the first-order perturbation terms that appear during the process of extracting H_{XY}^{23} and a single-qubit Hamiltonian H_0 from the original Hamiltonian H_q discussed in Sec. II D.

The first-order perturbation terms from the ideal Hamiltonian H_{XY}^{23} in five qubits are given by

$$H_{\mathrm{pert}} \approx -\sum_k 2\tau\{P^{(k)} + Q^{(k)} + R^{(k)}\}, \quad (B1)$$

where

$$
\begin{aligned}
P^{(k)} = {} & J_{12}^{(k-1)}\Omega_1^{(k-1)}Y_2^{(k-1)}Z_1^{(k-1)} + J_{34}^{(k-1)}\Omega_4^{(k-1)}Y_3^{(k-1)}Z_4^{(k-1)} \\
& + J_{45}^{(k-1)}\Omega_4^{(k-1)}Y_5^{(k-1)}Z_4^{(k-1)} \\
& + S_{\beta,1}^{(k)} + S_{\beta,4}^{(k)} + S_{\alpha,2}^{(k)} + S_{\alpha,3}^{(k)} + S_{\alpha,5}^{(k)}, \quad (B2)
\end{aligned}
$$

$$Q^{(k)} = J_{23}^{(k)}[\Omega_2^{(k)}Y_3^{(k)}Z_2^{(k)} + \Omega_3^{(k)}Y_2^{(k)}Z_3^{(k)}], \quad (B3)$$

$$
\begin{aligned}
R^{(k)} = {} & J_{12}^{(k)}\Omega_2^{(k)}Y_1^{(k)}Z_2^{(k)} + J_{34}^{(k)}\Omega_3^{(k)}Y_4^{(k)}Z_3^{(k)} + J_{45}^{(k)}\Omega_5^{(k)}Y_4^{(k)}Z_5^{(k)} \\
& + S_{\alpha,1}^{(k+1)} + S_{\alpha,4}^{(k+1)} + S_{\beta,2}^{(k+1)} + S_{\beta,3}^{(k+1)} + S_{\beta,5}^{(k+1)}, \quad (B4)
\end{aligned}
$$

where

$$S_{\alpha,i}^{(k)} = J_{ii}^{(k,k-1)}\Omega_i^{(k)}Y_i^{(k-1)}Z_i^{(k)}, \quad (B5)$$

$$S_{\beta,i}^{(k)} = J_{ii}^{(k,k-1)}\Omega_i^{(k-1)}Y_i^{(k)}Z_i^{(k-1)}. \quad (B6)$$

Thus, the perturbation terms can be described by

$$||H_{\mathrm{pert}}|| \approx 10\tau N_{\mathrm{qubit}}J\Omega, \quad (B7)$$

where N_{qubit} is the total number of qubits in a circuit. N_{qubit} is expressed by $N_{\mathrm{qubit}} = N_{\mathrm{logic}}N_{\mathrm{phys}}$ with the number of logical qubits N_{logic} and that of physical qubits in a logical qubit N_{phys}.

The first-order perturbation term to obtain the single-qubit Hamiltonian is given by

$$
\begin{aligned}
F_a^{(k)} = {} & J_{12}^{(k)}\Omega_1^{(k)}Y_2^{(k)}Z_1^{(k)} + [J_{23}^{(k)}Y_2^{(k)} + J_{34}^{(k)}Y_4^{(k)}]\Omega_3^{(k)}Z_3^{(k)} \\
& + J_{45}^{(k)}Y_4^{(k)}\Omega_5^{(k)}Z_5^{(k)}, \\
F_b^{(k)} = {} & [J_{12}^{(k)}Y_1^{(k)} + J_{23}^{(k)}Y_3^{(k)}]\Omega_2^{(k)}Z_2^{(k)} \\
& + [J_{34}^{(k)}Y_3^{(k)} + J_{45}^{(k)}Y_5^{(k)}]\Omega_4^{(k)}Z_4^{(k)}, \\
W_a^{(k)} = {} & S_{\alpha,1}^{(k)} + S_{\alpha,3}^{(k)} + S_{\alpha,5}^{(k)} + S_{\beta,1}^{(k+1)} + S_{\beta,3}^{(k+1)} + S_{\beta,5}^{(k+1)}, \\
W_b^{(k)} = {} & S_{\alpha,2}^{(k)} + S_{\alpha,4}^{(k)} + S_{\beta,2}^{(k+1)} + S_{\beta,4}^{(k+1)},
\end{aligned}
$$

$$
\begin{aligned}
H_{\mathrm{pert}} = {} & 2\tau\left\{\sum_k (-)^{k+1}\left(F_a^{(k)} + F_b^{(k)}\right)\right\} \\
& + \tau[8 + (-)^k 2]\left(-W_a^{(k)} + W_b^{(k)}\right). \quad (B8)
\end{aligned}
$$

Thus the perturbation terms can be estimated by

$$||H_{\mathrm{pert}}|| \approx 20\tau N_{\mathrm{qubit}}J\Omega. \quad (B9)$$

Equations (B7) and (B9) show that the number of connected qubits should be small so that the perturbation terms do not affect the main terms, even when we reduce the perturbation terms by using Eq. (24). Therefore, instead of connecting all qubits by an always-on Hamiltonian, it is better to divide qubits into several blocks such that the blocks are connected by some kind of switching mechanism [36–39].

[1] P. W. Shor, Phys. Rev. A **52**, R2493 (1995).

[2] A. Steane, Proc. R. Soc. London, Ser. A **452**, 2551 (1996).

[3] D. Gottesman, Ph.D. thesis, Caltech, 1997, arXiv:quant-ph/9705052.

[4] M. A. Nielsen and I. L. Chuang, *Quantum Computation and Quantum Information* (Cambridge University Press, Cambridge, 2000).

[5] A. M. Steane, Nature (London) **399**, 124 (1999).

[6] E. Knill, R. Laflamme, R. Martinez, and C. Negrevergne, Phys. Rev. Lett. **86**, 5811 (2001).

[7] J. Chiaverini, D. Leibfried, T. Schaetz, M. D. Barrett, R. B. Blakestad, J. Britton, W. M. Itano, J. D. Jost, E. Knill, C. Langer, R. Ozeri, and D. J. Wineland, Nature (London) **432**, 602 (2004).

[8] O. Moussa, J. Baugh, C. A. Ryan, and R. Laflamme, Phys. Rev. Lett. **107**, 160501 (2011).

[9] M. D. Reed, L. DiCarlo, S. E. Nigg, L. Sun, L. Frunzio, S. M. Girvin, and R. J. Schoelkopf, Nature (London) **482**, 382 (2012).

[10] D. Kribs, R. Laflamme, and D. Poulin, Phys. Rev. Lett. **94**, 180501 (2005).

[11] D. Poulin, Phys. Rev. Lett. **95**, 230504 (2005).

[12] D. Bacon, Phys. Rev. A **73**, 012340 (2006).

[13] A. Kitaev, Ann. Phys. **303**, 2 (2003); E. Dennis, A. Kitaev, A. Landahl, and J. Preskill, J. Math. Phys. **43**, 4452 (2002).

[14] H. Bombin, Phys. Rev. A **81**, 032301 (2010).

[15] S. Bravyi, B. M. Terhal, and B. Leemhuis, New J. Phys. **12**, 083039 (2010).

[16] R. Raussendorf and J. Harrington, Phys. Rev. Lett. **98**, 190504 (2007).

[17] P. Milman, W. Maineult, S. Guibal, L. Guidoni, B. Douot, L. Ioffe, and T. Coudreau, Phys. Rev. Lett. **99**, 020503 (2007).

[18] A. G. Fowler, M. Mariantoni, J. M. Martinis, and A. N. Cleland, Phys. Rev. A **86**, 032324 (2012).

[19] T. Tanamoto, D. Becker, V. M. Stojanović, and C. Bruder, Phys. Rev. A **86**, 032327 (2012).

[20] T. Tanamoto, V. M. Stojanović, C. Bruder, and D. Becker, Phys. Rev. A **87**, 052305 (2013).

[21] R. R. Ernst, G. Bodenhausen, and A. Wokaun, *Principles of Nuclear Magnetic Resonance in One and Two Dimensions* (Oxford University Press, Oxford, 1987).

[22] F. Schmidt-Kaler, H. Häffner, M. Riebe, S. Gulde, G. P. T. Lancaster, T. Deuschle, C. Becher, C. F. Roos, J. Eschner, and R. Blatt, Nature (London) **422**, 408 (2003).

[23] I. Roos and K. Mølmer, Phys. Rev. A **69**, 022321 (2004).

[24] C. D. Hill, Phys. Rev. Lett. **98**, 180501 (2007).

[25] B. T. Torosov, S. Guérin, and N. V. Vitanov, Phys. Rev. Lett. **106**, 233001 (2011).

[26] D. Becker, T. Tanamoto, A. Hutter, F. L. Pedrocchi, and D. Loss, Phys. Rev. A **87**, 042340 (2013).

[27] T. Yamamoto, Y. A. Pashkin, O. Astafiev, Y. Nakamura, and J. S. Tsai, Nature (London) **425**, 941 (2003).

[28] J. Q. You and F. Nori, Phys. Today **58**(11), 42 (2005).

[29] D. Loss and D. P. DiVincenzo, Phys. Rev. A **57**, 120 (1998).

[30] J. R. Petta, A. C. Johnson, J. M. Taylor, E. A. Laird, A. Yacoby, M. D. Lukin, C. M. Marcus, M. P. Hanson, and A. C. Gossard, Science **309**, 2180 (2005).

[31] B. E. Kane, Nature (London) **393**, 133 (1998).

[32] T. Tanamoto, Y. X. Liu, X. Hu, and F. Nori, Phys. Rev. Lett. **102**, 100501 (2009).

[33] J. Q. You, J. S. Tsai, and F. Nori, Phys. Rev. Lett. **89**, 197902 (2002).

[34] C. Rigetti, A. Blais, and M. Devoret, Phys. Rev. Lett. **94**, 240502 (2005).

[35] T. Tanamoto, Phys. Rev. A **64**, 062306 (2001).

[36] S. H. W. van der Ploeg, A. Izmalkov, A. M. van den Brink, U. Hübner, M. Grajcar, E. Il'ichev, H. G. Meyer, and A. M. Zagoskin, Phys. Rev. Lett. **98**, 057004 (2007).

[37] M. Grajcar, Y. X. Liu, F. Nori, and A. M. Zagoskin, Phys. Rev. B **74**, 172505 (2006).

[38] A. O. Niskanen, K. Harrabi, F. Yoshihara, Y. Nakamura, and J. S. Tsai, Phys. Rev. B **74**, 220503 (2006).

[39] S. Ashhab, S. Matsuo, N. Hatakenaka, and F. Nori, Phys. Rev. B **74**, 184504 (2006).

[40] R. J. Schoelkopf and S. M. Girvin, Nature (London) **451**, 664 (2008).

[41] J. Johansson, S. Saito, T. Meno, H. Nakano, M. Ueda, K. Semba, and H. Takayanagi, Phys. Rev. Lett. **96**, 127006 (2006).

[42] A. A. Houck, D. I. Schuster, J. M. Gambetta, J. A. Schreier, B. R. Johnson, J. M. Chow, L. Frunzio, J. Majer, M. H. Devoret, S. M. Girvin, and R. J. Schoelkopf, Nature (London) **449**, 328 (2007).

[43] H. Paik, D. I. Schuster, L. S. Bishop, G. Kirchmair, G. Catelani, A. P. Sears, B. R. Johnson, M. J. Reagor, L. Frunzio, L. I. Glazman, S. M. Girvin, M. H. Devoret, and R. J. Schoelkopf, Phys. Rev. Lett. **107**, 240501 (2011).

[44] A. Blais, R.-S. Huang, A. Wallraff, S. M. Girvin, and R. J. Schoelkopf, Phys. Rev. A **69**, 062320 (2004).

[45] V. M. Stojanović, A. Fedorov, A. Wallraff, and C. Bruder, Phys. Rev. B **85**, 054504 (2012).

[46] J. T. Barreiro, M. Muller, P. Schindler, D. Nigg, T. Monz, M. Chwalla, M. Hennrich, C. F. Roos, P. Zoller, and R. Blatt, Nature (London) **470**, 486 (2011).

[47] M. Steffen, Physics **4**, 103 (2011).

[48] Y. X. Liu, L. F. Wei, J. S. Tsai, and F. Nori, Phys. Rev. Lett. **96**, 067003 (2006).